



Article

Purification and Identification of an Antimicrobial Protein from *Bacillus stercoris* TY-12 and Its Biocontrol Functions Against *Ralstonia solanacearum*

Hui Wang^{1,2}, Jianqi Wei^{1,2}, Zhuoqing Yang^{1,2}, Tao Zhou^{1,2}, Mengdan Zhou^{1,2}, Yujing Xiao^{1,2}, Miaofang Chen^{1,2}, Wanrong Yang¹, Gaopeng Song^{1,2}, Hanhong Xu^{2,3} and Lei Wang^{1,2,*}

¹ Department of Chemical and Pharmaceutical Engineering, College of Materials and Energy, South China Agricultural University, Guangzhou 510642, China; pumpkinuu@163.com (H.W.); tianlangbingpo@163.com (J.W.); yangzhuoqing9974@163.com (Z.Y.); zhoutao0128@126.com (T.Z.); Zmd000923@163.com (M.Z.); yujingx2024@163.com (Y.X.); m15521169461@163.com (M.C.); 18718287941@163.com (W.Y.); songgp1021@scau.edu.cn (G.S.)

² National Key Laboratory of Green Pesticide, South China Agricultural University, Guangzhou 510642, China

³ College of Plant Protection, South China Agricultural University, Guangzhou 510642, China; hhxu@scau.edu.cn

* Correspondence: wanglei@scau.edu.cn; Tel.: +86-20-85285596

Abstract: *Ralstonia solanacearum* is a bacterial pathogen that causes bacterial wilt in plants, resulting in significant economic losses worldwide. Biological control that mainly utilizes *Bacillus* spp. is one of the most effective methods to prevent this disease. In this work, a strain of *Bacillus stercoris* TY-12 with an obvious antagonism effect on *R. solanacearum* was screened, and the inhibition diameter against *R. solanacearum* reached 2.18 cm by the plate antagonism test. Furthermore, an antimicrobial protein was isolated and purified from the fermentation supernatant of TY-12. The LC-MS/MS analysis results indicated that the purified antimicrobial protein is a member of the M42 family metalloproteinase with a molecular weight of approximately 40 kDa and named MP-TY12. After co-culture with MP-TY12 for 4 h, the cell surface of *R. solanacearum* was disrupted under SEM, indicating that MP-TY12 may inhibit *R. solanacearum* growth by enzymatically cleaving peptide bonds within the cell wall or membrane structure via hydrolysis. To evaluate the potential application of TY-12 in disease control during crop production, the biocontrol efficacy of TY-12 on the capsicum infected by *R. solanacearum* was investigated and achieved 84.18%. The growth promotion tests showed that the dry weight, fresh weight, stem diameter, stem length, root length, and the chlorophyll content of capsicum using TY-12 was obviously increased compared to the blank control. It is suggested that TY-12 could be used as a new biocontrol microbial strain in crop production and MP-TY12 might be developed as an antimicrobial agent.

Keywords: *Bacillus stercoris*; *Ralstonia solanacearum*; antimicrobial protein; metalloproteinase; biocontrol; crop protection



Academic Editor: Filomena Nazzaro

Received: 20 November 2024

Revised: 13 December 2024

Accepted: 26 December 2024

Published: 2 January 2025

Citation: Wang, H.; Wei, J.; Yang, Z.; Zhou, T.; Zhou, M.; Xiao, Y.; Chen, M.; Yang, W.; Song, G.; Xu, H.; et al.

Purification and Identification of an Antimicrobial Protein from *Bacillus stercoris* TY-12 and Its Biocontrol Functions Against *Ralstonia solanacearum*. *Appl. Microbiol.* **2025**, *5*, 2. <https://doi.org/10.3390/applmicrobiol5010002>

Copyright: © 2025 by the authors. Licensee MDPI, Basel, Switzerland. This article is an open access article distributed under the terms and conditions of the Creative Commons Attribution (CC BY) license (<https://creativecommons.org/licenses/by/4.0/>).

1. Introduction

Ralstonia solanacearum, recognized as one of the most devastating bacterial pathogens in plants, is a complex species with considerable diversity [1,2]. It can result in crop yield reductions ranging from 20% to 60%, posing a substantial threat to agricultural production [3,4]. Bacterial wilt caused by *R. solanacearum* initially prevalent in tropical and subtropical regions [5], has recently emerged in temperate and low-temperature areas [6],

potentially attributed to factors such as global warming, passive pathogen migration, and changes in crop cultivation systems. The occurrence of bacterial wilt in tomatoes is severe in the areas south of the Yangtze River in China, with disease incidence rates reaching up to 80% under favorable conditions [7]. *R. solanacearum* exhibits prolonged survival capabilities within the soil [8]. It can infiltrate root tissues through wounds or lateral root cracks and invade xylem vessels once contact with host plants [9–11]. The pathogen traverses the host's root system through flagellum-mediated motility [12,13], proliferates rapidly, and diffuses vertically within the plant via the vascular system while horizontally spreading to adjacent tissues [14–17]. This bacterium can secrete putrescine and extracellular polysaccharide (EPS), and cause the physical obstruction of xylem tissue, leading to leaf senescence, overall wilting of the plant, and eventual death [18–20].

Some classical methods against bacterial wilt are soil disinfection and resistant cultivar development [21,22]. Without the availability of an effective chemical control agent [23], biological control technology has emerged as a potent strategy for combating bacterial wilt, owing to its eco-friendly nature, efficacy, and environmental sustainability [24]. As an important biological control resource, *Bacillus* spp. has been widely used in controlling plant pathogens and producing novel biopesticides [25–28], which is related to its multifaceted biocontrol mechanisms including direct influence on pathogens, the regulation of plant physiological state, and immune response [25,29,30]. In a previous report, the biocontrol potential of *Bacillus subtilis*, *Bacillus amyloliquefaciens*, and *Stenotrophomonas maltophilia* in managing *Ralstonia* wilt on ginger was discovered [31]. Furthermore, it was demonstrated that natural compounds and *Bacillus subtilis* showed a synergistic effect in preventing papaya wilt [32], and volatile organic compounds produced by *Bacillus velezensis* FZB42 can reduce the virulence of *R. solanacearum* and inhibit its growth [33]. The ability of *Bacillus cereus* MH778713 against *Fusarium oxysporum* was evaluated and the potential of *B. cereus* MH778713 as a biocontrol agent was proposed [34]. With the considerable adjustment effects on plants at both physiological and molecular levels [35], *Bacillus* spp. with the ability to improve plant health and resilience directly or indirectly has become an important biocontrol agent in plant protection [36–39].

In this study, we screened and identified an antagonistic strain of *B. stercoris* TY-12 against *R. solanacearum* from the soil of muskmelon rhizosphere at Zengcheng Teaching and Research base, South China Agricultural University. We assessed the efficacy of TY-12 in controlling the capsicum bacterial wilt and its potential to promote capsicum growth. Then, the antimicrobial proteins in the fermentation supernatant of TY-12 were purified and identified by ammonium sulfate precipitation, DEAE, and LC-MS/MS. This research will contribute to providing effective biological agents for preventing and managing bacterial wilt in capsicums.

2. Materials and Methods

2.1. Isolation of Rhizobacteria

Five muskmelon rhizosphere soil samples with different levels of disease from mild to severe were collected from Zengcheng Teaching and Research Base, South China Agricultural University, with more than 40% of muskmelon suffering from wilt disease in this field. Then, 10^{-1} to 10^{-6} soil suspensions were prepared by serial dilution in sterile water and shaken at 37 °C, 150 r/min for 1 h on an orbital shaker (DZH-DA, HC, Taicang, China). The different gradient dilution suspensions were spread on an LB agar plate (1 L contained 10 g tryptone, 5 g yeast extract, 7 g NaCl, and 15 g agar, pH 7.0). Then, the LB plate was cultured at 37 °C for 1 day in a biochemical incubator (LRH-250, bluepard, Shanghai, China). According to the morphological characteristics of colonies, individual colonies with visible differences were isolated and cultured to obtain a purified strain [40].

All the purified strains were used for the subsequent screening of the antagonism of *R. solanacearum*.

2.2. Quantification of Antimicrobial Activity

The antagonistic strain against *R. solanacearum* was screened using the Oxford cup method [41]. Single colonies were taken for Gram staining and inoculated in 50 mL of LB broth and shaken for 24 h at 37 °C, 220 r/min to obtain the fermentation broth. The fermentation supernatant of strains was obtained by centrifuging the broth at 9500 × *g* for 2 min at 37 °C (D3024R, SCIOGEX, Rocky Hill, CT, USA); 20 µL of supernatant filtrate was added to each Oxford cup (diameter 6 mm), placed on an LB agar plate that contained 6% *R. solanacearum*, and sterile water was used as the negative control. Additionally, 1 mg/mL Ampicillin was used as the positive control. The plates were measured for inhibition zone after 48 h of incubation at 30 °C, and the experiment was replicated thrice.

2.3. Identification of Antagonistic Bacterium TY-12

The Omega Bacterial DNA Kit (D3350-01) was used to extract the genomic DNA of the strain TY-12, and the extracted DNA was used as a template to amplify the 16S rDNA fragment with universal primers 27F (5'-AGAGTTTGATCCTGGCTCAG-3') and 1492R (5'-GGTACCTTGTTACGACTT-3') [42]. The PCR system was composed of ddH₂O (16.25 µL), dNTPs Mixture (4 µL), 10× LA Taq Buffer II (2.5 µL), template DNA (1 µL), TaKaRa LA Taq (0.25 µL), upstream primer (0.5 µL), and downstream primer (0.5 µL). The PCR reaction program was as follows: 5 min of pre-denaturation at 94 °C, followed by 35 cycles of 30 s of denaturation at 94 °C, 30 s of annealing at 55 °C, and 1 min of extension at 72 °C, with a final extension of 10 min at 72 °C. The PCR products were detected by 1.2% agarose gel electrophoresis and sequenced by Beijing Tsingke Biotech Co., Ltd., Beijing, China. The sequence homology comparison was analyzed by BLAST tool of NCBI (<http://blast.ncbi.nlm.nih.gov/Blast.cgi> (accessed on 5 June 2023)). The phylogenetic tree was constructed by MEGA 11.0 software based on the 16S rDNA gene sequences of the strains, and evolutionary analysis was conducted using the neighbor-joining method.

2.4. Extraction and Purification of Antimicrobial Protein

The protein in the fermentation supernatant of the strain was separated by a series of ammonium sulfate (30%, 50%, 70%, and 90%) for about 8 h at each step. The precipitate was collected through centrifugation at 8512 × *g* and 4 °C for 30 min, dissolved in 0.02 mol/L Tris-HCl buffer (pH 7.6), and dialyzed using a 3.5 kDa filter at 4 °C for 8 h to remove (NH₄)₂SO₄. The antagonistic activity was assessed following the filter paper disc method [43]. The fraction exhibiting maximum antagonistic activity was further purified through diethyl-aminoethyl (DEAE) Sepharose fast flow anion exchange chromatography equilibrated with 0.02 mol/L Tris-HCl buffer (pH 7.6) and eluted by 0.02 mol/L Tris-HCl buffer with different concentrations of NaCl (0.2 M, 0.4 M, 1.0 M) [44]. The purified protein was analyzed by SDS-PAGE and the molecular weight was calibrated according to a prestained protein standard purchased from SMOBIO (Shanghai, China) [45].

2.5. Protein Concentration Determination

The protein concentration was calculated using the BCA method [46]. The concentration of each fraction was determined by Synergy 2 (BioTek, Winooski, VT, USA), and the procedure was referred to the BCA kit (Pierce™ BCA Protein Assay Kit, Prod # 23227, Waltham, MA, USA) instruction manual.

2.6. Identification of Antimicrobial Proteins

Peptide sequencing of the purified protein was carried out via LC-MS/MS. The project was entrusted to Shanghai Applied Protein Technology Co., Ltd., Shanghai, China. The purified protein was decomposed with trypsin enzyme and redissolved in 0.1% FA solution after being demineralized and lyophilized, and then analyzed using LC-MS/MS. The raw files were submitted to the MASCOT 2.7 software for further analysis, with searches conducted using the NCBI database.

2.7. Cell Surface Morphology Observation of *R. solanacearum*

MP-TY12 and *R. solanacearum* were co-cultured for 4 h to prepare the observation specimen. The specimen was first fixed with 2.5% glutaraldehyde in phosphate buffer (pH 7.0) for over 4 h and washed three times in the phosphate buffer. Then, the sample was postfixed with 1% OsO₄ in phosphate buffer (pH 7.0) for 1–2 h and washed three times in the phosphate buffer. After that, the specimen was dehydrated by a graded series of ethanol (30%, 50%, 70%, 80%, 90%, and 100%) for about 10 to 20 min at each step. Ultimately, the specimen was dehydrated in Leica Model CDP 300 critical point dryer with liquid CO₂. The dehydrated specimen was coated with platinum–palladium in Leica Model ACE 600 ion sputter and observed in ZEISS Model EVO MA 15 SEM (Thermo Fisher Scientific Model Verios 460 FESEM, Waltham, MA, USA).

2.8. Control Effect of TY-12 in Greenhouse

A quantity of full-bodied and homogeneous capsicum seeds, totaling ninety, were selected and planted within the seedling trays. The seeds were cultivated in a greenhouse for 6 weeks until they reached the four-leaf stage, and were divided into 3 experimental groups: CK (treated with water), Rs (injected with 10 mL *R. solanacearum* cell suspension with OD₆₀₀ as 1.0), and TY-12 + Rs (irrigated with 10 mL TY-12 cell suspension with OD₆₀₀ as 1.0 and injected 10 mL *R. solanacearum* cell suspension with OD₆₀₀ as 1.0 simultaneously); each group was repeated 3 times. The single plant disease incidence was recorded as 1 if observed and 0 if not after the seedlings were cultivated for another 2 weeks. The disease incidence rate was calculated by dividing the number of diseased seedlings by the total number of seedlings in the experimental group and multiplying by 100%. Symptoms of the capsicums at 8 weeks were classified into 5 levels: level 0, healthy seedlings with no symptoms; level 1, ≤25% of leaves were chlorosis or wilt; level 2, ≤50% of leaves were chlorosis or wilt; level 3, ≤75% of leaves were chlorosis or wilt; and level 4, more than 75% of leaves were chlorosis or wilt. The following formulas were used to calculate the disease index and control efficacy [47]:

$$DI = \left[\frac{\sum (\text{the seedling of ever grade} \times \text{relative grade})}{(\text{total seedlings} \times \text{the most serious grade})} \right] \times 100;$$

$$\text{Control efficacy (\%)} = \left[\frac{(\text{Disease index of control} - \text{Disease index of treated group})}{\text{Disease index of control}} \right] \times 100.$$

2.9. Growth-Promoting Effect of TY-12 in Greenhouse

A quantity of full-bodied and homogeneous capsicum seeds, totaling ninety, were selected and planted within the seedling trays, cultivated in a greenhouse for 2 weeks until they reached the two-leaf stage, and the seedlings were divided into 3 experimental groups: CK (treated with water), TY-12 (irrigated with 10 mL TY-12 cell suspension with OD₆₀₀ as 1.0), and 8-6 (irrigated with 10 mL *B. amyloliquefaciens* 8-6 cell suspension with OD₆₀₀ as 1.0); each group was repeated 3 times. The seedling was cultivated for another 2 weeks after being treated and the dry weight, fresh weight, stem diameter, stem length, root length, and chlorophyll content of the plants was measured.

2.10. Data Analysis

The 2.8 and 2.9 data were analyzed using the SPSS 27.0 statistics software. One-way analysis of variance (ANOVA) with LSD and Tukey's post hoc test was used to analyze the statistical significance of multiple groups.

3. Results

3.1. Inhibition of *R. solanacearum* by TY-12

The antagonistic activity of microorganisms originating from the soil of muskmelon rhizosphere with bacterial wilt was measured by the plate confrontation method. After 2 days of incubation, TY-12 exhibited antagonistic activity against *R. solanacearum* with a 2.18 cm inhibition diameter, which in the Ampicillin treatment group was 2.02 cm (Figure 1). The mean values were compared using an independent sample *t*-test. It was indicated that the antimicrobial activity against *R. solanacearum* of TY-12 was more than that of 1 mg/mL Ampicillin, and that TY-12 has potential application in biological control.

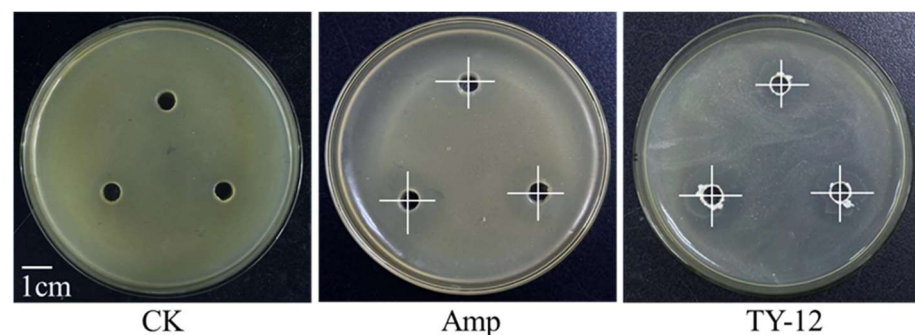


Figure 1. The antagonistic activity of *Bacillus stercoris* TY-12 against *R. solanacearum*. CK, ddH₂O; Amp, 1 mg/mL Ampicillin; TY-12, TY-12 fermentation supernatant. The amount of filtrate in each Oxford cup is 20 μ L.

3.2. Identification of TY-12

The 16S rDNA gene segment was cloned and sequenced to identify TY-12. The agarose gel electrophoresis analysis showed that the molecular weight of 16S rDNA of TY-12 was about 1500 bp (Figure 2C). The PCR amplification product of 16S rDNA was sequenced and analyzed by BLAST and showed 100% homology with the partial sequence of *B. stercoris* strain 22634 (OR432073.1). The results of the phylogenetic tree analysis indicated that TY-12 clustered with two strains of *B. stercoris*, leading to the identification of TY-12 as *B. stercoris* and named *B. stercoris* TY-12 (Figure 2D). The colonies of TY-12 were white on the LB culture medium with a rough texture and raised edges (Figure 2A), and the results in Figure 2B show that TY-12 is a Gram-positive bacterium.

3.3. Purification of the Antimicrobial Protein

The antimicrobial activity of *B. stercoris* TY-12 might be attributed to the antimicrobial molecule secreted by TY-12. In this work, the antimicrobial protein was isolated and purified by ammonium sulfate gradient precipitation and DEAE chromatography with antimicrobial activity screening. The results in Figure 3A,B show that the fraction of 50% ammonium sulfate precipitation had the best antimicrobial activity against *R. solanacearum*, with an inhibition diameter of 1.2 cm. The fraction of 30% ammonium sulfate precipitation exhibited an inhibition diameter of 0.8 cm, while the fractions of 70% and 90% ammonium sulfate precipitation did not produce inhibition zones. This indicates that antimicrobial protein may exist in the fraction of 50% ammonium sulfate precipitation, which was used for further purification.

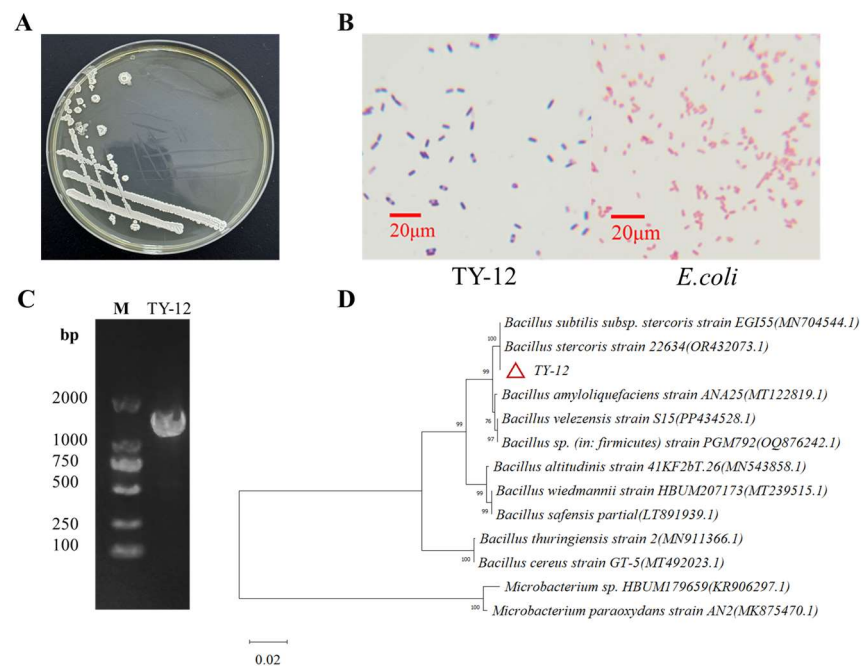


Figure 2. The colony morphology, Gram staining, agarose gel electrophoresis of TY-12 16s rDNA PCR product, and phylogenetic dendrogram based on 16S rDNA gene of strain TY-12. (A) Colony morphology of strain TY-12 on LB medium at 37 °C for 24 h. (B) Gram stains of TY-12 observed by Olympus microscope. (1000× magnification, *E. coli* was used as Gram-negative control, and TY-12 was Gram-positive). (C) PCR amplification of TY-12 16S rDNA genes. (D) Phylogenetic analysis of TY-12. The tree based on 16S rDNA gene sequences was constructed by the neighbor-joining method of MEGA 11.0 with bootstrap values based on 1000 replications, and the strain TY-12 is marked by triangle.

The 50% precipitate component was eluted into three fractions: the flow-through peak F1, fraction 2 (F2) eluted by 0.2 mol/L NaCl, and fraction 3 (F3) eluted by 0.4 mol/L NaCl through DEAE chromatography (Figure 3C). The results in Figure 3E indicate that F3 showed obvious antimicrobial activity with an inhibition diameter of 2.0 cm. It was found that F3 exhibited a relatively bright protein band with a molecular weight of approximately 40 kDa from SDS-PAGE electrophoresis analysis results (Figure 3D).

3.4. LC-MS/MS Analysis

The 40 kDa band of F3 in the SDS-PAGE electrophoresis was excised and the protein was identified by LC-MS/MS. The total ion flow result after enzymatic hydrolysis of the protein is shown in Figure 4A. A total of 106 unique peptides and 62 different proteins were identified by searching and analyzing the obtained mass spectrometry data, among which peptide coverages accounting for more than 5% are listed in Table 1. It was found that the molecular weight of the protein defined as M42 family metalloproteinase was consistent with the protein purified in this experiment after comparative analysis. The amino acid sequence of M42 family metalloproteinase was composed of 361 amino acids with a molecular weight of 39.3 kDa after NCBI data search, as shown in Figure 4B. As a result, we predicted that this protein is a kind of M42 family metalloproteinase named MP-TY12 and is responsible for the antimicrobial activity exhibited by the isolate.

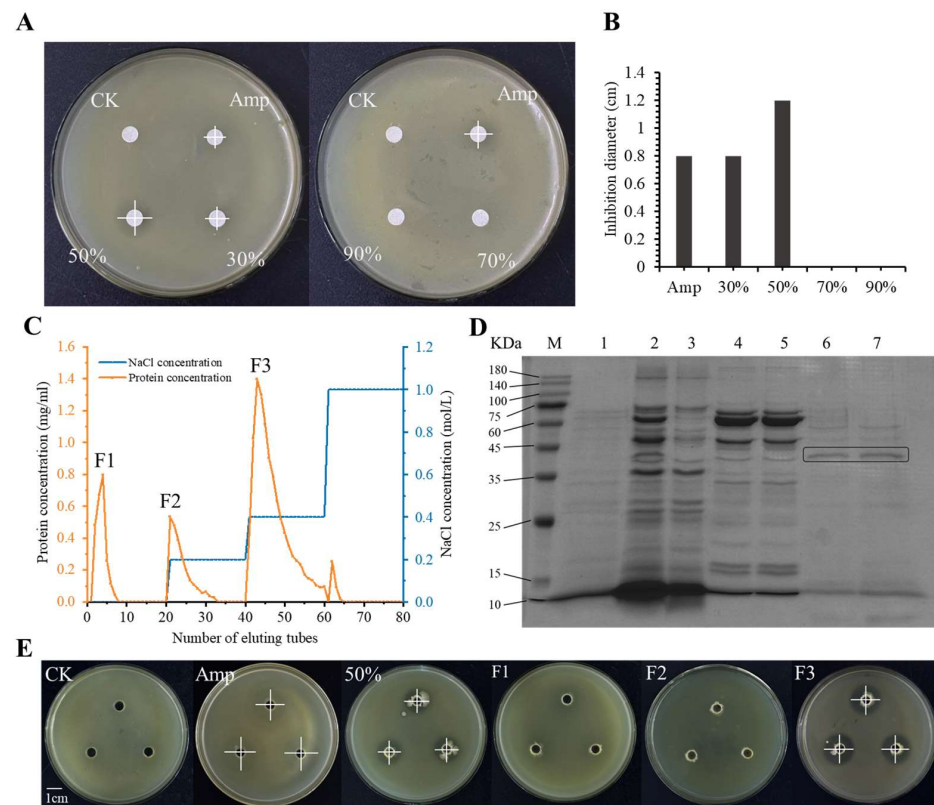


Figure 3. Purification and activity detection of antimicrobial protein from TY-12. (A) Inhibitory effects of crude proteins on *R. solanacearum* precipitated at various saturation levels of $(\text{NH}_4)_2\text{SO}_4$ (30%, 50%, 70%, 90%). The amount of 1 mg/mL Amp and protein on each filter paper is 20 μL . (B) The inhibition diameter of different ammonium sulfate precipitation components of TY12 fermentation supernatant. (C) Gradient elution curve of 50% TY-12 ammonium sulfate precipitated protein by DEAE Sepharose fast flow anion exchange chromatography. (D) SDS-PAGE analysis of elution fractions 1, 2, and 3 with different concentrations of NaCl. Lane 1, protein molecular mass marker; Lane 2, 50% ammonium sulfate precipitated protein; Lane 3, fraction 1 of unbound proteins; Lane 4 and Lane 5, fraction 2 eluted by 0.2 mol/L NaCl; Lane 6 and 7, fraction 3 eluted by 0.4 mol/L NaCl. (E) Inhibitory effects of different elution fractions on *R. solanacearum*. F1 was the flow-through peak of DEAE, F2 eluted by 0.2 mol/L NaCl, and F3 eluted by 0.4 mol/L NaCl.

Table 1. The partial identified proteins of fraction 3 (F3) by LC-MS/MS analysis with peptide coverage accounting for more than 5%.

Reference	Unique PepCount	Cover Percent	MW	PI
M42 family metalloproteinase (WP_071581572.1)	10	30.47%	39,288.64	5.84
serine protease (KFF56423.1)	7	21.27%	47,881.31	5.2
dihydrolipoyl dehydrogenase (BEV37900.1)	6	10.64%	49,732.21	4.95
catalase (KFF57258.1)	4	7.87%	54,751.52	6
aminopeptidase YwaD (WP_151257520.1)	4	5.05%	49,306.26	6

3.5. Effect of Antimicrobial Protein on *R. solanacearum* Cell Surface

Cellular morphological changes of *R. solanacearum* caused by MP-TY12 were evaluated by scanning electron microscopy. Figure 5A shows that *R. solanacearum* is a rod-shaped bacterium. After being treated with MP-TY12, the cells of *R. solanacearum* were fractured compared to the control under the 12,000 \times microscope (Figure 5B) Under the 80,000 \times microscope, the cell was swelled, ruptured, and appeared in irregular shapes with depressions on the surface. Based on the results, we speculate that MP-TY12 may inhibit *R. solanacearum*

3.6. Control Effect of TY-12 Against *R. solanacearum* in Capsicum

We conducted a greenhouse pot experiment to assess the ability of TY-12 to control bacterial wilt in capsicums. The results in Figure 6A show that the capsicum leaves injected with *R. solanacearum* were yellow with yellowish-brown spots and the capillary roots were less than that of the blank control, while the roots were more developed and the stem was thicker and higher in the experiment group of capsicums co-treated by TY-12 and *R. solanacearum*. It was found that the capsicum plants stunted and wilted when inoculated with *R. solanacearum* singly, while the disease symptoms of wilting were mild in the group co-treatment by TY-12 and *R. solanacearum*, and the plants were taller and stronger than the CK and Rs groups (Figure 6B).

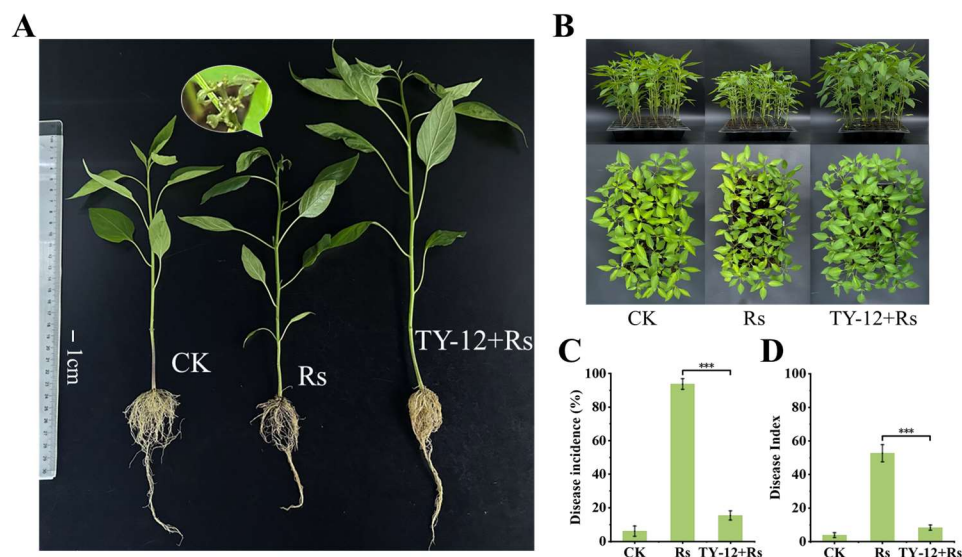


Figure 6. *B. stercoris* TY-12 reduced the pathogenicity of *R. solanacearum* in capsicum. (A,B) Capsicums treated for 2 weeks with CK (water), Rs (*R. solanacearum* cell suspension with OD_{600} as 1.0), and TY-12 + Rs (*B. stercoris* TY-12 cell suspension with OD_{600} as 1.0 and injected 10 mL *R. solanacearum* cell suspension with OD_{600} as 1.0 simultaneously). A represents the difference of a single capsicum plant, and B shows the growth of the capsicum in the seedling tray. (C) Disease incidence of bacterial wilt with different treatments. (D) Disease index of bacterial wilt with different treatments. Different asterisks indicate the significant difference between treatments; ***, $p < 0.001$.

The disease incidence rate and disease index were calculated, and the results in Figure 6C,D show that the disease incidence rate in the Rs group approached 93.6% and decreased to 15.5% in the TY-12 and *R. solanacearum* co-treated group. At the same time, the disease index (DI) in the Rs group was 52.65 and significantly reduced to 8.33 in the group co-treatment by TY-12 and *R. solanacearum*, and the control efficacy of TY-12 against bacterial wilt was 84.18%.

3.7. Effect of *B. stercoris* TY-12 on Capsicum Growth

We explored the effect of *B. stercoris* TY-12 on the growth of capsicum. Two-week-old capsicum seedlings were irrigated with TY-12 and *Bacillus amyloliquefaciens* 8-6 bacterial fermentation broth. The plant growth status was recorded 2 weeks later (Figure 7A). Compared with the control (water), the dry weight (Figure 7B), fresh weight (Figure 7C), stem diameter (Figure 7D), stem length (Figure 7E), and root length (Figure 7F) of capsicum was significantly increased by TY-12 and was higher than that of *B. amyloliquefaciens* 8-6 (positive control group). The chlorophyll content of leaves was obviously increased by TY-12 treatment (Figure 7G). It was indicated that TY-12 had a significant promoting effect on the growth of capsicum plants.

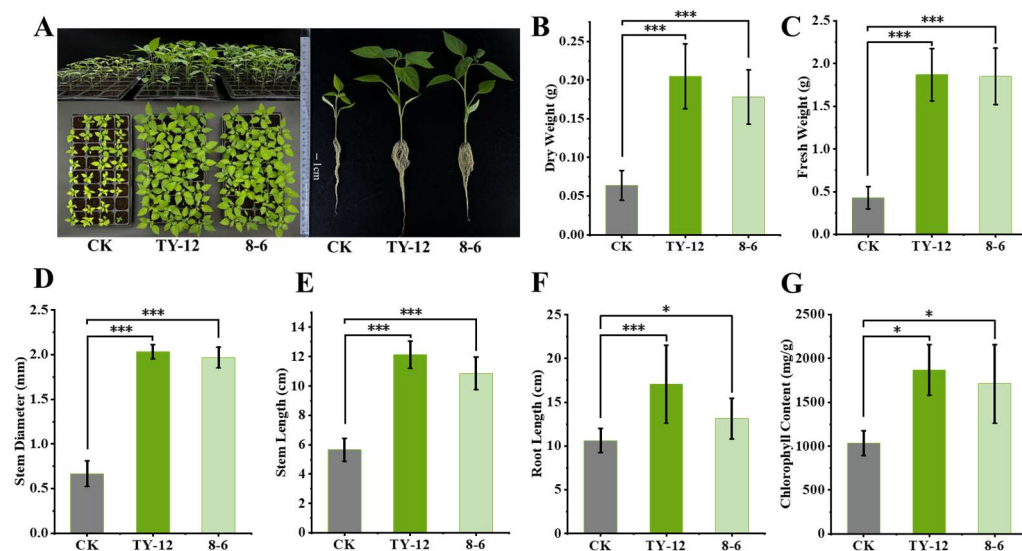


Figure 7. *B. stercoris* TY-12 promoted capsicum growth. (A) Capsicums treated for 2 weeks with CK (water), TY-12 (*B. stercoris* TY-12 cell suspension with OD₆₀₀ as 1.0), and 8-6 (*B. amyloliquefaciens* cell suspension with OD₆₀₀ as 1.0). The capsicum plant growth status of dry weight (B), fresh weight (C), stem diameter (D), stem length (E), root length (F), and chlorophyll content (G) were measured. Different asterisks indicate the significant difference between treatments; *, $p < 0.05$; ***, $p < 0.001$.

4. Discussion

Bacterial wilt is widespread and difficult to control. Biological control has been proposed as a sustainable and effective method for preventing and treating bacterial wilt. According to published reports, some strains of *Bacillus* spp., *Pantoea* spp., and *Pseudomonas* spp. have a certain effect on the prevention and control of bacterial wilt [48–51]. Some bacteria and fungi in the plant rhizosphere can enhance the plant's defense and improve the immune system's sensitivity. In diseased plants, the abundance of the antagonistic bacteria may increase and activate the plant's resistance to the pathogen [52,53].

As naturally occurring microorganisms, *Bacillus* spp. can decompose organic matter and release nutrients for crop uptake and utilization, while improving soil texture and structure [54]. The application of these species as plant growth-promoting rhizobacteria in agriculture has many advantages [55–57], such as the production of a variety of antimicrobial compounds and the induction of plant resistance [58–61].

Bacillus stercoris is considered a subspecies of *Bacillus subtilis* and was promoted to species status recently, and is generally considered environmentally friendly as a plant rhizobacteria [62,63]. From the pot results of this study, it was speculated that *B. stercoris* TY-12 may produce a range of antibiotic compounds, including M42 family metallopeptidase, to enhance the resistance of plants to *R. solanacearum* and decrease the severity of the disease [64,65]. With great antimicrobial stability in multiple plate tests, TY-12 can reach 10⁹ CFU/mL after 24 h of cultivation in LB medium, making it inexpensive. TY-12's favorable plant growth-promoting effects lay the foundation for its application as a novel agricultural biocontrol agent.

Even though *Bacillus* spp. has been widely recognized and used as a probiotic, we still need to be cautious about its safety [66]. To determine whether TY-12 is completely safe for use as a microbial agent, further microbiological tests, toxicity tests, and agricultural relevance evaluations are still required to be explored.

Metallopeptidases are defined as hydrolases with bivalent metal cation-mediated activity, and metals have a special effect on the hydrolysis and activity of the peptidases [67–69]. It was reported that metallopeptidases are involved in the activation of biological path-

ways [70,71]. In this study, we speculate that the antimicrobial protein MP-TY12 may be a zinc-dependent metallopeptidase, demonstrating the potential of metallopeptidase for the biological control in bacterial wilt [72].

About M42 family metallopeptidase, previous research demonstrated that M42 family member TET peptidase is a strict glycyl aminopeptidase that lacks amidolytic activity toward other types of amino acids [73], and multiple structures and mechanisms of latency in metallopeptidase zymogens have also been reported [74], like the structure and evolution of astacin metallopeptidases being described [75]. However, the mechanism by which M42 family metallopeptidases inhibit the growth of *R. solanacearum* remains unclear. We speculate that M42 family metallopeptidases may affect the growth and reproduction of *R. solanacearum* by catalyzing the hydrolysis of proteins or peptides and participating in a variety of biological processes. Furthermore, metallopeptidase might diminish the proliferation rate and reproductive capacity of *R. solanacearum* by hydrolyzing proteins or peptides associated with its metabolic pathway and disrupting its regular physiological functions. In conclusion, further investigation and discourse are still required to elucidate and explore these mechanisms' precise functionalities and interdependencies.

5. Conclusions

B. stercoris TY-12 can inhibit the growth of *R. solanacearum* in vitro. Through the isolation, purification, and identification of its antimicrobial proteins, we obtained a kind of M42 family metallopeptidase. Pot experiments demonstrated that *B. stercoris* TY-12 enhanced the resistance of capsicum plants to capsicum bacterial wilt, achieving a control efficacy of 84.18%. Furthermore, the fermentation broth of *B. stercoris* TY-12 exhibited a beneficial growth-promoting effect on capsicum plants.

Author Contributions: Conceptualization, H.W. and L.W.; validation, Z.Y., T.Z., M.Z., and Y.X.; writing—original draft preparation, H.W.; writing—review and editing, J.W., W.Y., M.C. and M.Z.; supervision, L.W., G.S. and H.X.; visualization, H.W., J.W. and M.C. All authors have read and agreed to the published version of the manuscript.

Funding: This work was supported by the Guangzhou Rural Science and Technology Commissioner Project (GZKTP20191); The Blue Fire Plan Industry University Research Project of Ministry of Education (CXZJHZ201712); The National Natural Science Foundation of China (82073722); and Guangdong Basic and Applied Basic Research Foundation (2022A1515010016).

Data Availability Statement: The original contributions presented in the study are included in the article, further inquiries can be directed to the corresponding author.

Conflicts of Interest: The authors declare no conflicts of interest.

References

1. Su, Y.X.; Xu, Y.N.; Li, Q.Q.; Yuan, G.Q.; Zheng, D.H. The essential genome of *Ralstonia solanacearum*. *Microbiol. Res.* **2020**, *238*, 126500. [[CrossRef](#)] [[PubMed](#)]
2. Singh, N. *Ralstonia solanacearum*: An emerging threat as a mysterious plant pathogen. *Curr. Sci.* **2021**, *120*, 20–21.
3. Wang, Z.J.; Luo, W.B.; Cheng, S.J.; Zhang, H.J.; Zong, J.; Zhang, Z. *Ralstonia solanacearum*—A soil borne hidden enemy of plants: Research development in management strategies, their action mechanism and challenges. *Front. Plant Sci.* **2023**, *14*, 1141902. [[CrossRef](#)] [[PubMed](#)]
4. Castillo, J.A.; Greenberg, J.T. Evolutionary dynamics of *Ralstonia solanacearum*. *Appl. Environ. Microbiol.* **2007**, *73*, 1225–1238. [[CrossRef](#)]
5. Li, C.Y.; Hu, W.C.; Pan, B.; Liu, Y.; Yuan, S.F.; Ding, Y.Y.; Li, R.; Zheng, X.Y.; Shen, B.; Shen, Q.R. Rhizobacterium *Bacillus amyloliquefaciens* strain SQRT3-mediated induced systemic resistance controls bacterial wilt of tomato. *Pedosphere* **2017**, *27*, 1135–1146. [[CrossRef](#)]
6. Genin, S.; Boucher, C. Lessons learned from the genome analysis of *Ralstonia solanacearum*. *Annu. Rev. Phytopathol.* **2004**, *42*, 107–134. [[CrossRef](#)]

7. Liu, Y.; Wu, D.; Liu, Q.; Zhang, S.; Tang, Y.; Jiang, G.; Li, S.; Ding, W. The sequevar distribution of *Ralstonia solanacearum* in tobacco-growing zones of China is structured by elevation. *Eur. J. Plant Pathol.* **2017**, *147*, 541–551. [[CrossRef](#)]
8. Zhu, Y.J.; Xiao, R.F.; Liu, B. Growth and pathogenicity characteristics of *Ralstonia solanacearum* strain RS1100 in long-term stationary phase culture. *J. Plant Dis. Prot.* **2010**, *117*, 156–161. [[CrossRef](#)]
9. Genin, S. Molecular traits controlling host range and adaptation to plants in. *New Phytol.* **2010**, *187*, 920–928. [[CrossRef](#)]
10. Hendrich, C.G.; Truchon, A.N.; Dalsing, B.L.; Allen, C. Nitric oxide regulates the *Ralstonia solanacearum* type III secretion system. *Mol. Plant-Microbe Interact.* **2023**, *36*, 334–344. [[CrossRef](#)] [[PubMed](#)]
11. Hamilton, C.D.; Steidl, O.R.; MacIntyre, A.M.; Hendrich, C.G.; Allen, C. *Ralstonia solanacearum* depends on catabolism of myo-inositol, sucrose, and trehalose for virulence in an infection stage-dependent manner. *Mol. Plant-Microbe Interact.* **2021**, *34*, 669–679. [[CrossRef](#)]
12. Tans-Kersten, J.; Huang, H.; Allen, C. *Ralstonia solanacearum* needs motility for invasive virulence on tomato. *J. Bacteriol.* **2001**, *183*, 3597–3605. [[CrossRef](#)] [[PubMed](#)]
13. Wang, Y.; Xian, L.; Yu, G.; Macho, A.P. Tomato stem injection for the precise assessment of *Ralstonia solanacearum* fitness in planta. *Bio-Protocol* **2021**, *11*, e4134. [[CrossRef](#)] [[PubMed](#)]
14. Khokhani, D.; Tuan, T.M.; Lowe-Power, T.M.; Allen, C. Plant assays for quantifying *Ralstonia solanacearum* virulence. *Bio-Protocol* **2018**, *8*, e3028. [[CrossRef](#)]
15. Lowe-Power, T.M. Metabolic Analyses of *Ralstonia Solanacearum* During Plant Pathogenesis. Ph.D. Thesis, University of Wisconsin—Madison, Madison, WI, USA, 2017.
16. Xu, C.H.; Zhong, L.K.; Huang, Z.M.; Li, C.Y.; Lian, J.Z.; Zheng, X.F.; Liang, Y. Real-time monitoring of *Ralstonia solanacearum* infection progress in tomato and arabidopsis using bioluminescence imaging technology. *Plant Methods* **2022**, *18*, 7. [[CrossRef](#)] [[PubMed](#)]
17. Liu, Y.; Tan, X.; Cheng, H.J.; Gong, J.; Zhang, Y.; Wang, D.B.; Ding, W. The cold shock family gene *cspD3* is involved in the pathogenicity of *Ralstonia solanacearum* CQPS-1 to tobacco. *Microb. Pathog.* **2020**, *142*, 104091. [[CrossRef](#)]
18. Lowe-Power, T.M.; Hendrich, C.G.; von Roepenack-Lahaye, E.; Li, B.; Wu, D.S.; Mitra, R.; Dalsing, B.L.; Ricca, P.; Naidoo, J.; Cook, D.; et al. Metabolomics of tomato xylem sap during bacterial wilt reveals *Ralstonia solanacearum* produces abundant putrescine, a metabolite that accelerates wilt disease. *Environ. Microbiol.* **2018**, *20*, 1330–1349. [[CrossRef](#)]
19. Denny, T.P. *Ralstonia solanacearum*—A plant pathogen in touch with its host. *Trends Microbiol.* **2000**, *8*, 486–489. [[CrossRef](#)]
20. Shen, F.F.; Yin, W.F.; Song, S.H.; Zhang, Z.H.; Ye, P.Y.; Zhang, Y.; Zhou, J.N.; He, F.; Li, P.; Deng, Y.Y. *Ralstonia solanacearum* promotes pathogenicity by utilizing l-glutamic acid from host plants. *Mol. Plant Pathol.* **2020**, *21*, 1099–1110. [[CrossRef](#)]
21. Horita, M.; Kobara, Y.; Yano, K.; Hayashi, K.; Nakamura, Y.; Iiyama, K.; Oki, T. Comprehensive control system for ginger bacterial wilt disease based on anaerobic soil disinfestation. *Agronomy* **2023**, *13*, 1791. [[CrossRef](#)]
22. Bittner, R.J.; Arellano, C.; Mila, A.L. Effect of temperature and resistance of tobacco cultivars to the progression of bacterial wilt, caused by *Ralstonia solanacearum*. *Plant Soil* **2016**, *408*, 299–310. [[CrossRef](#)]
23. Yuliar, Nion, Y.A.; Toyota, K. Recent trends in control methods for bacterial wilt diseases caused by *Ralstonia solanacearum*. *Microbes Environ.* **2015**, *30*, 1–11. [[CrossRef](#)]
24. Elnahal, A.S.M.; El-Saadony, M.T.; Saad, A.M.; Desoky, E.-S.M.; El-Tahan, A.M.; Rady, M.M.; AbuQamar, S.F.; El-Tarabily, K.A. The use of microbial inoculants for biological control, plant growth promotion, and sustainable agriculture: A review. *Eur. J. Plant Pathol.* **2022**, *162*, 759–792. [[CrossRef](#)]
25. Etesami, H.; Jeong, B.R.; Glick, B.R. Biocontrol of plant diseases by *Bacillus* spp. *Physiol. Mol. Plant Pathol.* **2023**, *126*, 102048. [[CrossRef](#)]
26. Serrão, C.P.; Ortega, J.C.G.; Rodrigues, P.C.; de Souza, C.R.B. *Bacillus* species as tools for biocontrol of plant diseases: A meta-analysis of twenty-two years of research, 2000–2021. *World J. Microbiol. Biotechnol.* **2024**, *40*, 110. [[CrossRef](#)]
27. Karačić, V.; Miljaković, D.; Marinković, J.; Ignjatov, M.; Milošević, D.; Tamindžić, G.; Ivanović, M. *Bacillus* Species: Excellent biocontrol agents against tomato diseases. *Microorganisms* **2024**, *12*, 457. [[CrossRef](#)] [[PubMed](#)]
28. Dimkić, I.; Janakiev, T.; Petrović, M.; Degrassi, G.; Fira, D. Plant-associated *Bacillus* and *Pseudomonas* antimicrobial activities in plant disease suppression via biological control mechanisms—A review. *Physiol. Mol. Plant Pathol.* **2022**, *117*, 101754. [[CrossRef](#)]
29. Grahovac, J.; Pajčin, I.; Vlajkov, V. *Bacillus* VOCs in the context of biological control. *Antibiotics* **2023**, *12*, 581. [[CrossRef](#)]
30. Zhang, N.; Wang, Z.; Shao, J.; Xu, Z.; Liu, Y.; Xun, W.; Miao, Y.; Shen, Q.; Zhang, R. Biocontrol mechanisms of *Bacillus*: Improving the efficiency of green agriculture. *Microb. Biotechnol.* **2023**, *16*, 2250–2263. [[CrossRef](#)] [[PubMed](#)]
31. Yang, W.; Xu, Q.; Liu, H.-X.; Wang, Y.-P.; Wang, Y.-M.; Yang, H.-T.; Guo, J.-H. Evaluation of biological control agents against *Ralstonia* wilt on ginger. *Biol. Control* **2012**, *62*, 144–151. [[CrossRef](#)]
32. Hossain, M.F.; Billah, M.; Ali, M.R.; Parvez, M.S.A.; Zaoti, Z.F.; Hasan, S.M.Z.; Hasan, M.F.; Dutta, A.K.; Khalekuzzaman, M.; Islam, M.A.; et al. Molecular identification and biological control of *Ralstonia solanacearum* from wilt of papaya by natural compounds and *Bacillus subtilis*: An integrated experimental and computational study. *Saudi J. Biol. Sci.* **2021**, *28*, 6972–6986. [[CrossRef](#)]

33. Tahir, H.A.S.; Ali, Q.; Rajer, F.U.; Shakeel, Q.; Gillani, W.; Binyamin, R.; Tayyab, H.M.A.; Khan, A.R.; Gu, Q.; Gao, X.W.; et al. Transcriptomic analysis of *Ralstonia solanacearum* in response to antibacterial volatiles of *Bacillus velezensis* FZB42. *Arch. Microbiol.* **2023**, *205*, 358. [[CrossRef](#)] [[PubMed](#)]
34. Ramírez, V.; Martínez, J.; Bustillos-Cristales, M.d.R.; Catañeda-Antonio, D.; Munive, J.-A.; Baez, A. *Bacillus cereus* MH778713 elicits tomato plant protection against *Fusarium oxysporum*. *J. Appl. Microbiol.* **2022**, *132*, 470–482. [[CrossRef](#)]
35. Pii, Y.; Mimmo, T.; Tomasi, N.; Terzano, R.; Cesco, S.; Crecchio, C. Microbial interactions in the rhizosphere: Beneficial influences of plant growth-promoting rhizobacteria on nutrient acquisition process. A review. *Biol. Fertil. Soils* **2015**, *51*, 403–415. [[CrossRef](#)]
36. Zhang, C.; Wang, M.-Y.; Khan, N.; Tan, L.-L.; Yang, S. Potentials, utilization, and bioengineering of plant growth-promoting methylobacterium for sustainable agriculture. *Sustainability* **2021**, *13*, 3941. [[CrossRef](#)]
37. Xu, J.; Qin, L.; Xu, X.; Shen, H.; Yang, X. *Bacillus paralicheniformis* RP01 enhances the expression of growth-related genes in cotton and promotes plant growth by altering microbiota inside and outside the root. *Int. J. Mol. Sci.* **2023**, *24*, 7227. [[CrossRef](#)] [[PubMed](#)]
38. Della Mónica, I.F.; Wong Villarreal, A.; Stefanoni Rubio, P.J.; Vaca-Paulín, R.; Yañez-Ocampo, G. Exploring plant growth-promoting rhizobacteria as stress alleviators: A methodological insight. *Arch. Microbiol.* **2022**, *204*, 316. [[CrossRef](#)] [[PubMed](#)]
39. Adedayo, A.A.; Babalola, O.O.; Prigent-Combaret, C.; Cruz, C.; Stefan, M.; Kutu, F.; Glick, B.R. The application of plant growth-promoting rhizobacteria in *Solanum lycopersicum* production in the agricultural system: A review. *PeerJ* **2022**, *10*, e13405. [[CrossRef](#)]
40. Testa, M.M.; Ruiz de Valladares, R.; Benito de Cardenas, I.L. Antagonistic interactions among *Fusobacterium nucleatum* and *Prevotella intermedia* with oral *Lactobacilli*. *Res. Microbiol.* **2003**, *154*, 669–675. [[CrossRef](#)]
41. Sun, G.; Yao, T.; Feng, C.; Chen, L.; Li, J.; Wang, L. Identification and biocontrol potential of antagonistic bacteria strains against *Sclerotinia sclerotiorum* and their growth-promoting effects on *Brassica napus*. *Biol. Control* **2017**, *104*, 35–43. [[CrossRef](#)]
42. Yang, R.; Ye, W.; Liu, P.; Li, J.; Lu, M.; Wang, Z.; Shao, D. Endophytic *Bacillus amyloliquefaciens* Mdg15 is a potential biocontrol agent against tree peony gray mold caused by *Botrytis cinerea*. *Eur. J. Plant Pathol.* **2024**, *169*, 431–445. [[CrossRef](#)]
43. Saravanakumar, D.; Thomas, A.; Banwarie, N. Antagonistic potential of lipopeptide producing *Bacillus amyloliquefaciens* against major vegetable pathogens. *Eur. J. Plant Pathol.* **2019**, *154*, 319–335. [[CrossRef](#)]
44. Ren, J.; He, W.; Li, C.; He, S.; Niu, D. Purification and identification of a novel antifungal protein from *Bacillus subtilis* XB-1. *World J. Microbiol. Biotechnol.* **2019**, *35*, 150. [[CrossRef](#)]
45. Hashmi, S.; Iqbal, S.; Ahmed, I.; Janjua, H.A. Production, optimization, and partial purification of alkali-thermotolerant proteases from newly isolated *Bacillus subtilis* S1 and *Bacillus amyloliquefaciens* KSM12. *Processes* **2022**, *10*, 1050. [[CrossRef](#)]
46. Lozzi, I.; Pucci, A.; Pantani, O.L.; D'Acqui, L.P.; Calamai, L. Interferences of suspended clay fraction in protein quantitation by several determination methods. *Anal. Biochem.* **2008**, *376*, 108–114. [[CrossRef](#)] [[PubMed](#)]
47. Shan, Y.; Wang, D.; Zhao, F.-H.; Song, J.; Zhu, H.; Li, Y.; Zhang, X.-J.; Dai, X.-F.; Han, D.; Chen, J.-Y. Insights into the biocontrol and plant growth promotion functions of *Bacillus altitudinis* strain KRS010 against *Verticillium dahliae*. *BMC Biol.* **2024**, *22*, 116. [[CrossRef](#)]
48. Abo-Elyousr, K.A.M.; Hassan, S.A. Biological control of *Ralstonia solanacearum* (Smith), the causal pathogen of bacterial wilt disease by using *Pantoea* spp. *Egypt. J. Biol. Pest Control* **2021**, *31*, 113. [[CrossRef](#)]
49. Chen, D.; Liu, X.; Li, C.; Tian, W.; Shen, Q.; Shen, B. Isolation of *Bacillus amyloliquefaciens* S20 and its application in control of eggplant bacterial wilt. *J. Environ. Manag.* **2014**, *137*, 120–127. [[CrossRef](#)] [[PubMed](#)]
50. Sun, Y.; Su, Y.; Meng, Z.; Zhang, J.; Zheng, L.; Miao, S.; Qin, D.; Ruan, Y.; Wu, Y.; Xiong, L.; et al. Biocontrol of bacterial wilt disease in tomato using *Bacillus subtilis* strain R31. *Front. Microbiol.* **2023**, *14*, 1281381. [[CrossRef](#)] [[PubMed](#)]
51. Suansia, A.; Senapati, A.K.; Samantaray, D.; Mohanty, M.K. Evaluation of antagonistic activity of DAPG-producing fluorescent *Pseudomonads* from rhizospheres of solanaceous crops for biocontrol of bacterial wilt. *J. Phytopathol.* **2024**, *172*, e13315. [[CrossRef](#)]
52. Pieterse, C.M.J.; Zamioudis, C.; Berendsen, R.L.; Weller, D.M.; Van Wees, S.C.M.; Bakker, P.A.H.M. Induced systemic resistance by beneficial microbes. *Annu. Rev. Phytopathol.* **2014**, *52*, 347–375. [[CrossRef](#)] [[PubMed](#)]
53. Yu, K.; Liu, Y.; Tichelaar, R.; Savant, N.; Lagendijk, E.; van Kuijk, S.J.L.; Stringlis, I.A.; van Dijken, A.J.H.; Pieterse, C.M.J.; Bakker, P.A.H.M.; et al. Rhizosphere-Associated *Pseudomonas* suppress local root immune responses by gluconic acid-mediated lowering of environmental pH. *Curr. Biol.* **2019**, *29*, 3913–3920. [[CrossRef](#)]
54. Yang, W. Components of rhizospheric bacterial communities of barley and their potential for plant growth promotion and biocontrol of *Fusarium* wilt of watermelon. *Braz. J. Microbiol.* **2019**, *50*, 749–757. [[CrossRef](#)] [[PubMed](#)]
55. Ye, M.; Tang, X.; Yang, R.; Zhang, H.; Li, F.; Tao, F.; Li, F.; Wang, Z. Characteristics and application of a novel species of *Bacillus*: *Bacillus velezensis*. *ACS Chem. Biol.* **2018**, *13*, 500–505. [[CrossRef](#)] [[PubMed](#)]
56. Bach, E.; Seger, G.D.d.S.; Fernandes, G.d.C.; Lisboa, B.B.; Passaglia, L.M.P. Evaluation of biological control and rhizosphere competence of plant growth promoting bacteria. *Appl. Soil Ecol.* **2016**, *99*, 141–149. [[CrossRef](#)]
57. Roriz, M.; Pereira, S.I.A.; Castro, P.M.L.; Carvalho, S.M.P.; Vasconcelos, M.W. Impact of soybean-associated plant growth-promoting bacteria on plant growth modulation under alkaline soil conditions. *Heliyon* **2023**, *9*, e14620. [[CrossRef](#)]

58. Shen, S.; Yu, F.; Hao, X.; Chen, J.; Gao, H.; Lai, X. A novel *Bacillus* sp. with antagonistic activity against a plant pathogen, *Fusarium graminearum*, and its potential antagonistic mechanism. *Lett. Appl. Microbiol.* **2023**, *76*, ovad098. [[CrossRef](#)]
59. Saengchan, C.; Sangpueak, R.; Le Thanh, T.; Phansak, P.; Buensanteai, N. Induced resistance against *Fusarium solani* root rot disease in cassava plant (*Manihot esculenta* Crantz) promoted by salicylic acid and *Bacillus Subtilis*. *Acta Agric. Scand. Sect. B Soil Plant Sci.* **2022**, *72*, 516–526. [[CrossRef](#)]
60. Gowtham, H.G.; Murali, M.; Singh, S.B.; Lakshmeesha, T.R.; Narasimha Murthy, K.; Amruthesh, K.N.; Niranjana, S.R. Plant growth promoting rhizobacteria- *Bacillus amyloliquefaciens* improves plant growth and induces resistance in chilli against anthracnose disease. *Biol. Control* **2018**, *126*, 209–217. [[CrossRef](#)]
61. Cao, Y.; Pi, H.; Chandransu, P.; Li, Y.; Wang, Y.; Zhou, H.; Xiong, H.; Helmann, J.D.; Cai, Y. Antagonism of two plant-growth promoting *Bacillus velezensis* isolates against *Ralstonia solanacearum* and *Fusarium oxysporum*. *Sci. Rep.* **2018**, *8*, 4360. [[CrossRef](#)] [[PubMed](#)]
62. Dunlap, C.A.; Bowman, M.J.; Zeigler, D.R. Promotion of *Bacillus subtilis* subsp. *inaquosorum*, *Bacillus subtilis* subsp. *spizizenii* and *Bacillus subtilis* subsp. *stercoris* to species status. *Antonie Van Leeuwenhoek* **2020**, *113*, 1–12. [[CrossRef](#)] [[PubMed](#)]
63. Wang, B.; Peng, H.; Wu, W.; Yang, B.; Chen, Y.; Xu, F.; Peng, Y.; Qin, Y.; Fu, P.; Lu, J. Genomic insights into biocontrol potential of *Bacillus stercoris* LJBS06. *3 Biotech* **2021**, *11*, 458. [[CrossRef](#)]
64. Chen, M.C.; Wang, J.P.; Zhu, Y.J.; Liu, B.; Yang, W.J.; Ruan, C.Q. Antibacterial activity against *Ralstonia solanacearum* of the lipopeptides secreted from the *Bacillus amyloliquefaciens* strain FJAT-2349. *J. Appl. Microbiol.* **2019**, *126*, 1519–1529. [[CrossRef](#)]
65. Chandwani, S.; Dewala, S.; Chavan, S.M.; Paul, D.; Pachaiappan, R.; Gopi, M.; Amaresan, N. Complete genome sequencing of *Bacillus subtilis* (CWTS 5), a siderophore-producing bacterium triggers antagonistic potential against *Ralstonia solanacearum*. *J. Appl. Microbiol.* **2023**, *134*, lxad066. [[CrossRef](#)]
66. Todorov, S.D.; Ivanova, I.V.; Popov, I.; Weeks, R.; Chikindas, M.L. *Bacillus* spore-forming probiotics: Benefits with concerns? *Crit. Rev. Microbiol.* **2022**, *48*, 513–530. [[CrossRef](#)] [[PubMed](#)]
67. Smith, E.L. The mode of action of the metal-peptidases*. *Proc. Natl. Acad. Sci. USA* **1949**, *35*, 80–90. [[CrossRef](#)]
68. Gossas, T.; Danielson, U.H. Characterization of Ca²⁺ interactions with matrix metalloproteinase-12: Implications for matrix metalloproteinase regulation. *Biochem. J.* **2006**, *398*, 393–398. [[CrossRef](#)]
69. Vargas Rigo, G.; Gomes Cardoso, F.; Bongiorno Galego, G.; da Rosa, D.F.; dos Santos, A.L.; Tasca, T. Metalloproteinases as key virulence attributes of clinically relevant protozoa: New discoveries, perspectives, and frontiers of knowledge. *Curr. Protein Pept. Sci.* **2023**, *24*, 307–328. [[CrossRef](#)] [[PubMed](#)]
70. Gómez, M.; Gutiérrez, M.S.; González, A.M.; Gárate-Castro, C.; Sepúlveda, D.; Barahona, S.; Baeza, M.; Cifuentes, V.; Alcaíno, J. Metalloproteinase Stp1 activates the transcription factor Sre1 in the carotenogenic yeast *Xanthophyllomyces dendrorhous*. *J. Lipid Res.* **2020**, *61*, 229–243. [[CrossRef](#)]
71. Potok, P.; Zawada, M.; Potocki, S. Determination of the role of specific amino acids in the binding of Zn(II), Ni(II), and Cu(II) to the active site of the M10 family metalloproteinase. *J. Inorg. Biochem.* **2024**, *253*, 112500. [[CrossRef](#)]
72. Jongeneel, C.V.; Bouvier, J.; Bairoch, A. A unique signature identifies a family of zinc-dependent metalloproteinases. *FEBS Lett.* **1989**, *242*, 211–214. [[CrossRef](#)]
73. Basbous, H.; Appolaire, A.; Girard, E.; Franzetti, B. Characterization of a glycyl-specific TET aminopeptidase complex from *Pyrococcus horikoshii*. *J. Bacteriol.* **2018**, *200*, e00059-18. [[CrossRef](#)] [[PubMed](#)]
74. Arolas, J.L.; Goulas, T.; Cuppari, A.; Gomis-Rüth, F.X. Multiple architectures and mechanisms of latency in metalloproteinase zymogens. *Chem. Rev.* **2018**, *118*, 5581–5597. [[CrossRef](#)]
75. Gomis-Rüth, F.X.; Stöcker, W. Structural and evolutionary insights into astacin metalloproteinases. *Front. Mol. Biosci.* **2023**, *9*, 1080836. [[CrossRef](#)] [[PubMed](#)]

Disclaimer/Publisher's Note: The statements, opinions and data contained in all publications are solely those of the individual author(s) and contributor(s) and not of MDPI and/or the editor(s). MDPI and/or the editor(s) disclaim responsibility for any injury to people or property resulting from any ideas, methods, instructions or products referred to in the content.